

## v-SNARE-dependent secretion is required for phagocytosis

DAVID J. HACKAM\*<sup>†</sup>, ORI D. ROTSTEIN<sup>†</sup>, CAROLA SJOLIN\*<sup>†</sup>, ALAN D. SCHREIBER<sup>‡</sup>, WILLIAM S. TRIMBLE\*,  
AND SERGIO GRINSTEIN\*<sup>§</sup>

\*Division of Cell Biology, Hospital for Sick Children, Toronto, Ontario, M5G 1X8 Canada; <sup>†</sup>Department of Surgery, The Toronto Hospital, Toronto, Ontario, M5G 2C4 Canada; and <sup>‡</sup>Department of Medicine, University of Pennsylvania, Philadelphia, PA 10104-4283

Edited by William E. Paul, National Institutes of Health, Bethesda, MD, and approved August 14, 1998 (received for review March 6, 1998)

**ABSTRACT** Phagosomes are generally believed to form by gradual apposition of the plasma membrane of leukocytes onto the surface of invading microorganisms. The internalization of the encapsulated particle is therefore predicted to reduce the surface area of the phagocyte. Contrary to this prediction, we observed that phagocytosis is associated with a net increase in cell surface area, suggesting the concomitant occurrence of exocytosis. Selective cleavage of components of the secretory machinery by microinjection or transfection of bacterial neurotoxins induced a pronounced inhibition of phagocytosis. These observations indicate that vesicle-soluble *N*-ethylmaleimide-sensitive factor attachment protein receptor-mediated exocytosis of endomembranes is essential for optimal completion of particle internalization during phagocytosis.

Phagocytosis of microorganisms by leukocytes is an essential component of the host defense against infection. Microbes are initially engulfed by extensions of the plasmalemma and become internalized into a membrane-bound vacuole, the phagosome, which subsequently matures upon fusion with endosomes and lysosomes (1–3). It is generally believed that the vacuole is created by “zippering” of the plasmalemma around the surface of the microorganism, followed by fusion at the point where the enveloping membranes make contact (4, 5). This assumes that the membrane of the forming phagosome is derived from a portion of the existing plasma membrane, which would likely result in a net reduction in surface area of the cell, limiting the size and number of particles internalized. However, the observation that macrophages can ingest multiple particles suggests a process whereby replenishment of the plasma membrane occurs during phagocytosis. Fusion of intracellular membrane pools with the cell surface could provide a mechanism to reconcile this apparent discrepancy with the “zipper” hypothesis. In this regard, activation of phagocytic cells has been reported to be associated with delivery of endomembranes to the plasma membrane. Buys *et al.* (6) showed that upon stimulation by phorbol esters, macrophages undergo a 66% increase in surface area, which correlated with the appearance of endosomal markers on the plasma membrane.

Recent studies have shed light on the mechanisms governing vesicle secretion in a variety of systems. Regulated exocytosis requires the formation of a core complex consisting of a vesicular membrane protein such as vesicle-associated membrane protein 2 (VAMP-2; also called synaptobrevin) and two proteins found in the plasma membrane, syntaxin and soluble *N*-ethylmaleimide-sensitive factor (NSF) attachment protein (SNAP) 25 (synaptosome-associated protein). This tripartite complex then serves as the receptor for the soluble proteins NSF and SNAP (7–11). Some of these proteins are susceptible

to proteolysis by specific clostridial neurotoxins, which are therefore potent and selective inhibitors of exocytosis. VAMP and a related vesicular SNAP receptor (v-SNARE), cellubrevin, are effectively and selectively degraded by tetanus toxin and botulinum toxin B (12, 13). The specificity of the toxins toward the v-SNAREs has been convincingly demonstrated by a number of approaches, including mutational analysis (14).

In the current studies, we utilized clostridial neurotoxins to investigate the role of exocytosis in the process of phagocytosis. The results indicate that optimal completion of phagocytosis requires the incorporation of endomembranes to the plasmalemma and that this process is regulated by v-SNAREs.

### MATERIALS AND METHODS

**Materials, Antibodies, and Solutions.** Texas red-labeled zymosan, NHS-biotin, avidin-fluorescein isothiocyanate, FM-143, Lucifer yellow, FITC, rhodamine-labeled human holotransferrin, tetramethylrhodamine B isothiocyanate, and Texas red-dextran were obtained from Molecular Probes. Sheep erythrocytes (SRBCs) and goat anti-sheep erythrocyte IgG were purchased from ICN. Botulinum toxin from *Clostridium botulinum* was obtained from List Biological Laboratories (Campbell, CA). Latex particles (1- and 3- $\mu$ m diameter), desiccated *Micrococcus lysodeikticus*, donkey serum, and Hepes-buffered medium RPMI were obtained from Sigma. Human IgG was obtained from Baxter Healthcare Corp. (Glendale, CA). A polyclonal antibody to VAMP-2 was raised against a peptide corresponding to the N-terminal 15 amino acids as described (15). Aggregated human IgG was prepared as described (16) and then labeled with tetramethylrhodamine B isothiocyanate (1 mg/ml). Cy3-conjugated donkey anti-rabbit IgG was obtained from Jackson ImmunoResearch.

Tetanus toxin light chain (TeTx-LC) cDNA was obtained from H. Niemann (Institut für Biochemie Medizinische Hochschule, Hannover, Germany), and recombinant His6-tagged protein was purified as described (14). Proteolytic activity and specificity of the recombinant toxin were confirmed by demonstrating cleavage of a single 18-kDa VAMP-2 immunoreactive band on SDS/PAGE in total membranes obtained from brain and J774 cells (15).

PBS consisted of 140 mM NaCl, 10 mM KCl, 8 mM sodium phosphate, and 2 mM potassium phosphate (pH 7.4). Microinjection buffer consisted of 110 mM potassium acetate, 20 mM NaCl, 10 mM Hepes, 2 mM MgCl<sub>2</sub>, and 1 mM DTT (pH 7.2).

This paper was submitted directly (Track II) to the *Proceedings* office. Abbreviations: VAMP-2, vesicle-associated membrane protein 2; NSF, *N*-ethylmaleimide-sensitive factor; SNARE, soluble NSF attachment protein (SNAP) receptor; v-SNARE, vesicle SNARE; TeTx-LC, tetanus toxin light chain; SRBC, sheep red blood cell; OPZ, opsonized zymosan; CHO, Chinese hamster ovary; GFP, green fluorescence protein; FITC, fluorescein isothiocyanate.

<sup>§</sup>To whom reprint requests should be addressed at: Division of Cell Biology, Hospital for Sick Children, 555 University Ave., Toronto, Ontario, M5G 1X8 Canada. e-mail: sga@sickkids.on.ca.

The publication costs of this article were defrayed in part by page charge payment. This article must therefore be hereby marked “advertisement” in accordance with 18 U.S.C. §1734 solely to indicate this fact.

© 1998 by The National Academy of Sciences 0027-8424/98/9511691-6\$2.00/0  
PNAS is available online at www.pnas.org.

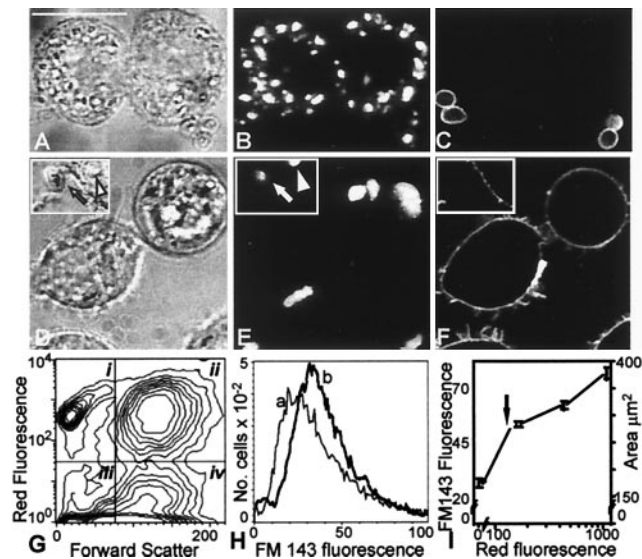


FIG. 1. Changes in macrophage surface area after phagocytosis of OPZ. (A–C) J774 cells were allowed to interact with biotinylated, Texas red-labeled OPZ. Extracellular particles were identified by treatment with avidin-FITC. (A) Bright field (Nomarski) image. Bar, 10  $\mu\text{m}$ . (B) Red fluorescence (Texas red emission) of cells in A as analyzed by confocal fluorescence microscopy, indicating the location of OPZ. (C) Green fluorescence (avidin-FITC emission) of cells in A, identifying extracellular OPZ. (D–F) J774 cells were allowed to internalize Texas red-labeled OPZ as in A, treated with the dye FM-143 at 4°C (which provides a measure of the surface membrane), and then examined by confocal microscopy. (D) Bright field image; inset shows an extracellular particle (arrow) and an intracellular particle (arrowhead). (E) Red (Texas red) fluorescence of cells in D indicating the location of OPZ. (F) Green (FM-143) fluorescence indicating surface labeling of cell only. (G) Analysis of association of OPZ with J774 cells by flow cytometry. The arbitrarily designated quadrants define the following populations: i, extracellular OPZ; ii, macrophages with associated OPZ; iii, debris; and iv, macrophages not associated with OPZ. (H) Frequency histogram of the fluorescence intensity of cell-associated FM-143, a measure of cell surface area. The lighter line (a) corresponds to cells in quadrant iv in G, which had no associated OPZ. The heavy line (b) corresponds to cells in quadrant ii in G, which had internalized OPZ. (I) Correlation between Texas red fluorescence (abscissa), which is proportional to the number of OPZ particles (fluorescence equivalent to one internalized particle shown by arrow) and the uptake of FM-143 (left ordinate), which is proportional to surface area (calculated from the volume of cells, assuming a smooth spherical surface; right ordinate). Data from five separate experiments.

**Cell Culture and Handling.** The murine cell line J774 was obtained from American Type Culture Collection. Chinese hamster ovary (CHO) cells were stably transfected with Fc $\gamma$ RIIA cDNA, yielding Fc $\gamma$ RIIA-CHO cells (17). Both cell lines were maintained in DMEM with 10% fetal bovine serum and 5% penicillin-streptomycin (Life Technologies, Grand Island, NY) and incubated at 37°C under 5% CO<sub>2</sub>. Prior to microinjection, cells were plated overnight on acid-washed glass coverslips at a density of 10<sup>5</sup> cells/well.

cDNAs encoding TeTx-LC or green fluorescent protein (GFP) in pcDNA3.1 were purified as described (14). Fc $\gamma$ RIIA-CHO cells were maintained in DMEM containing 10% serum and 1 mg/ml G418. For transfections, cells were plated overnight onto glass coverslips to 15% confluence and transfected with 2  $\mu\text{g}$  of GFP cDNA, with or without 5  $\mu\text{g}$  of TeTx-LC cDNA, using calcium phosphate (18).

**Microinjection and Immunofluorescence Microscopy.** For microinjection, cells were transferred to a Leiden coverslip holder and bathed in Hepes-buffered RPMI. Microinjection was performed using pipettes pulled from filament-containing borosilicate capillaries with an inner diameter of 0.78 mm using

a Flaming/Brown model P87 micropipette puller (Sutter Instruments, Navato, CA). TeTx-LC or botulinum toxin (1  $\mu\text{mol/liter}$ ) and either Lucifer yellow (1 mg/ml) or FITC-dextran (1 mg/ml) were dissolved in microinjection buffer. Solutions were injected into the cytoplasm of cells using a micromanipulator (Model 5171) and injector (Model 5246, Eppendorf) under phase-contrast microscopy (19). A volume equivalent to approximately 10% of the total cell volume was injected. After microinjection, cells were incubated in fresh medium at 37°C for 5 h.

For VAMP-2 immunofluorescence, cells were fixed for 3 h with 4% paraformaldehyde in PBS at 23°C and washed in 100 mM glycine-PBS for 10 min. The cells were then permeabilized with 0.1% Triton X-100 in PBS for 20 min at 23°C, washed in ice-cold PBS, and blocked for 1 h with 5% donkey serum in PBS at 23°C. After washing in PBS, coverslips were incubated with a 1:200 anti-VAMP-2 in 1% albumin-PBS for 1 h at 23°C. Coverslips were washed three times with cold PBS, treated with a 1:1000 dilution of Cy3-labeled anti-rabbit antibody for 1 h at 4°C, and mounted using Slow Fade (Molecular Probes). Fluorescence was analyzed using a Leica Model TCS4D (Heidelberg, Germany) laser confocal microscope. Microinjected cells were identified by detecting the fluorescence of Lucifer yellow with excitation at 450 nm, while Cy3 fluorescence was visualized at 540 nm. The mean radius of zymosan particles was calculated by comparing Nomarski images with polystyrene spheres of known diameter. Cells were sized electronically using the Coulter Channelyzer and also microscopically. Composites of confocal images were assembled and labeled using Photoshop and Illustrator software (Adobe Systems, Mountain View, CA). All experiments were performed at least four times. Representative images are displayed where appropriate.

**Assessment of Phagocytosis, Endocytosis, Surface Area, and Adherence.** Two methods were used for assessment of phagocytosis. Cells were exposed to biotinylated, IgG-opsionized Texas red-labeled zymosan particles at 37°C for the times indicated below. Particles were biotinylated in 1 mg/ml *N*-hydroxysuccinimide-biotin for 1 h at 37°C. Where indicated, particles were then opsonized for 1 h at 37°C with either 1 mg/ml of human IgG or serum obtained from individuals with agammaglobulinemia. Particles were then incubated for 45 min at 37°C with J774 cells that had been plated overnight on glass coverslips. Extracellular opsonized zymosan (OPZ) was removed by briefly incubating the cells in 0.25% trypsin-EDTA followed by thorough washing in cold PBS. Cells were fixed with 4% paraformaldehyde and treated with avidin-FITC (1:1000) to identify extracellular adherent particles. The second method used SRBCs that were opsonized with goat anti-sheep erythrocyte IgG (1:10, 1 h 37°C) and then washed in cold PBS to remove unbound IgG. SRBCs were added to plated J774 cells ( $\approx 10$  SRBCs/cell) in medium containing 10% serum and incubated for 1 h at 37°C. Extracellular SRBCs were removed by hypotonic lysis (water, 30 sec). Internalized SRBCs were quantified under Nomarski optics.

To evaluate changes in surface area during phagocytosis, adherent J774 cells which had internalized Texas red-labeled OPZ, were scraped into ice-cold PBS, washed three times, resuspended at 10<sup>6</sup> cells/ml, and placed on ice. Control cells were not exposed to OPZ. Cells were treated with FM-143 (1 mM) on ice for 5 min and examined by confocal microscopy to confirm that the dye labeled only the cell surface (20). Bound FM-143 fluorescence was quantified by flow cytometry. The fluorescence of Texas red-labeled-OPZ was measured to establish the number of particles associated with macrophages. Over 90% of the cell-associated OPZ particles were not accessible to extracellularly added avidin, implying that they had undergone phagocytosis.

For determination of fluid-phase endocytosis, J774 cells were allowed to internalize Texas red-dextran (1 mg/ml) for 2 h at 37°C. To determine receptor-mediated endocytosis,

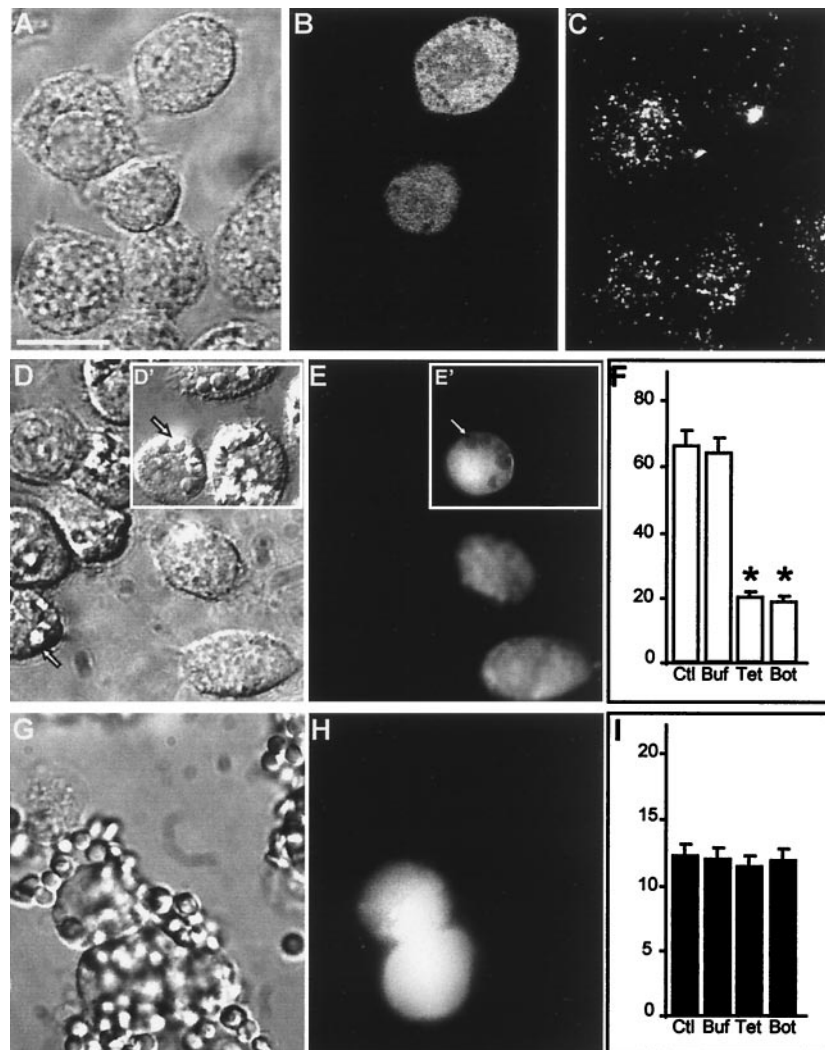


FIG. 2. Impaired phagocytosis after degradation of VAMP-2 in J774 cells. (A–C) J774 cells were injected with TeTx-LC in a solution containing fixable FITC-dextran as a marker of injection. After 5 h of incubation at 37°C, the cells were stained with antibody to VAMP-2. (A) Bright field micrograph. Bar, 10  $\mu$ m. (B) Green fluorescence (Lucifer yellow emission) of the field shown in A identifying two injected cells. (C) VAMP-2 immunostaining in the cells shown in A. (D–F) J774 cells were injected with tetanus toxin and FITC-dextran as above, then assessed for their ability to perform phagocytosis of opsonized SRBCs. (D) Bright field micrograph. Inset (D') shows cell injected with dextran alone. Arrow indicates location of representative internalized SRBCs. (E and E') Green fluorescence emission of the cells shown in D. Arrowhead demonstrates the displacement of FITC-dextran by internalized SRBCs. (F) Effect of toxin injection on phagocytosis. Data are means  $\pm$  SE of 250 noninjected control (Ctl) cells, 175 buffer- (Buf) injected controls, 244 TeTx-LC- (Tet) injected cells, and 75 botulinum- (Bot) injected cells (asterisks indicate  $P < 0.05$  vs. Ctl). (G–I) J774 cells were injected with TeTx-LC as above and then assessed for their ability to bind opsonized SRBCs. (G) Bright field micrograph. (H) Fluorescence emission of the cells shown in G identifying injected cells. (I) Effect of toxin injection on SRBC adherence to J774 cells. Data are means  $\pm$  SE of 165 noninjected control (Ctl) cells, 64 buffer- (Buf) injected controls, 75 TeTx-LC- (Tet) injected cells, and 57 botulinum- (Bot) injected cells. Images are representative of five separate experiments.

Fc $\gamma$ R1IA-CHO cells were incubated with either rhodamine-labeled transferrin (25  $\mu$ g/ml) or tetramethylrhodamine B isothiocyanate-labeled aggregated human IgG for 1 h at 37°C. Cells were then washed in cold PBS, fixed in 4% paraformaldehyde, and examined by confocal microscopy. Endocytosis was quantified by analyzing the digital images using MetaMorph software (Universal Imaging, Media, PA).

To assess particle adherence, J774 cells or Fc $\gamma$ R1IA-CHO cells were incubated with opsonized SRBCs for 30 min at 4°C. Nonadhered SRBCs were removed by washing in PBS, and the number of bound SRBCs/macrophage was quantified under light microscopy.

## RESULTS

**Changes in Membrane Surface Area Accompanying Phagocytosis.** We first examined the changes in the membrane surface area that accompany phagocytosis of yeast particles

(zymosan) by J774 macrophages (Fig. 1). J774 cells were allowed to internalize OPZ, under conditions which resulted in the association of multiple intracellular particles per macrophage. Most of the particles that remain associated with the cells after washing were not accessible to extracellularly added avidin, indicating that they were indeed engulfed, as opposed to merely adhered to the surface of the macrophages (Fig. 1, A–C). The approximate area of membrane internalized during the course of phagocytosis could be estimated from the size and number of zymosan particles taken up per cell, assuming a tight apposition with the phagosomal membrane. For cells such as those in Fig. 1 that took up  $\approx 10$  particles, this area is roughly 94  $\mu$ m<sup>2</sup>/cell, which is equivalent to 62% of the original surface area of J774 cells, estimated from electronic volume measurements, assuming a smooth spherical shape. These calculations imply that, either the surface membrane is much greater than estimated from geometric considerations (due perhaps to the presence of ruffles or other protrusions), or that

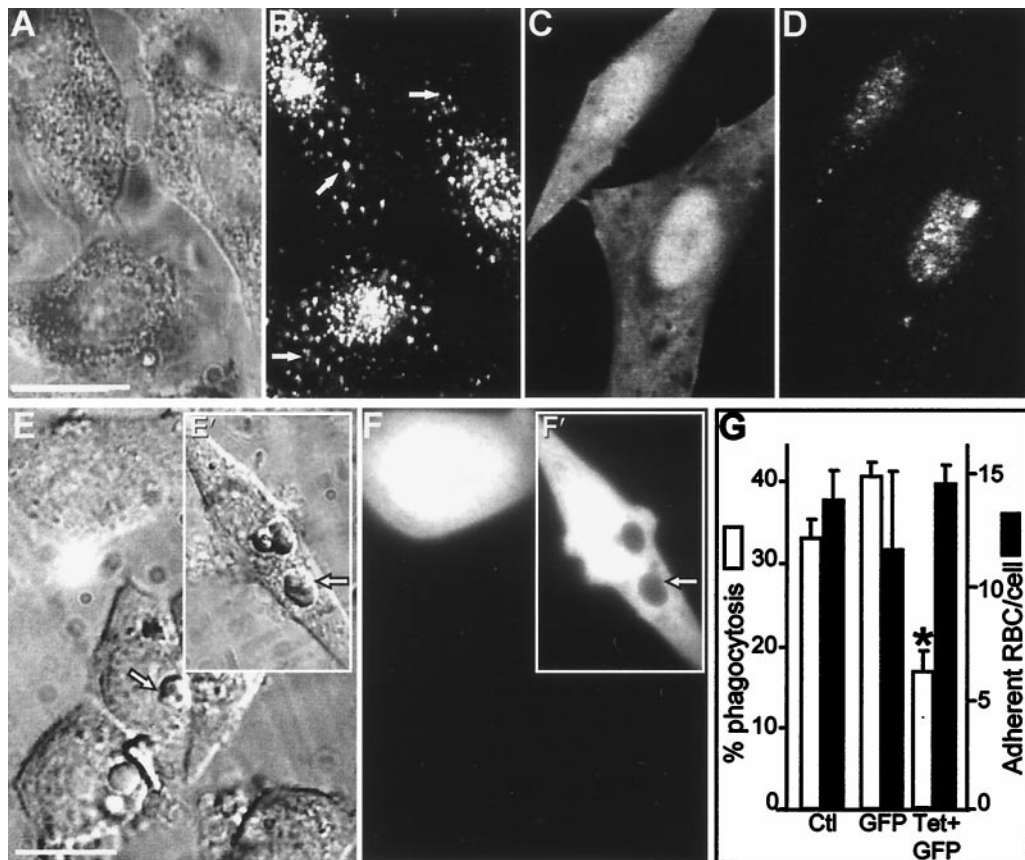


FIG. 3. Impaired phagocytosis after degradation of VAMP-2 in Fc $\gamma$ RIIA-transfected CHO cells. (A and B) VAMP-2 immunostaining of CHO cells. (A) Nomarski image. (B) VAMP-2 immunostaining in the cells shown in A. Arrows indicate specific, vesicular staining. (C and D) Fc $\gamma$ RIIA-expressing CHO cells were transiently transfected with cDNA-encoding TeTx-LC, along with cDNA for GFP as a transfection marker, and immunostained with antibody to VAMP-2. (C) Green (GFP) fluorescence identifying transfected cells. (D) VAMP-2 immunostaining of cells shown in C. (E and F) Fc $\gamma$ RIIA-expressing CHO cells were cotransfected with TeTx-LC and GFP as above and allowed to internalize opsonized SRBCs. (E) Bright field image. *Inset* (E') shows cells transfected with GFP alone. Arrowhead indicates location of representative internalized SRBCs. (F and F') GFP fluorescence identifying transfected cells in the field shown in E. The arrowhead demonstrates the displacement of GFP by internalized SRBCs in cells transfected with GFP alone. (G) Effect of TeTx-LC expression on phagocytosis and adherence of SRBCs by Fc $\gamma$ RIIA-CHO cells. Means  $\pm$  SE of five individual experiments, with more than 200 cells per group per experiment. Asterisks indicate  $P < 0.05$  vs. control (Ctl). Bar, 10  $\mu$ m.

internal membranes are recruited to the plasmalemma to compensate for the loss incurred during phagocytosis.

To more accurately estimate the surface membrane before and after phagocytosis, we used the impermeant, solvochromic dye FM-143, which becomes fluorescent when intercalated into the outer leaflet of the plasmalemma (20). Phagocytosis was induced as in Fig. 1A–C and cells were cooled to 4°C and exposed to FM-143 to quantify the area of the plasmalemma. Confocal microscopy confirmed that under these conditions, the dye was confined to the plasma membrane (Fig. 1D–F). Flow cytometric analysis revealed that over 50% of the macrophages were associated with Texas red-labeled OPZ (Fig. 1E). Unexpectedly, the surface area of cells that had taken up yeast particles, identified by their red fluorescence, was greater than that of cells that had not been exposed to zymosan (Fig. 1H). In fact, the increase in macrophage surface area correlated directly with the number of particles internalized (Fig. 1I). These observations suggest that formation of phagosomes is accompanied by the insertion of endomembranes into the plasmalemma.

**Effects of v-SNARE Degradation on Phagocytosis.** Membrane addition may occur independently of phagocytosis to maintain homeostasis of the surface area. Alternatively, exocytosis may occur at the time and site of phagocytosis, to deliver additional membrane surface that may be essential for the formation of the phagosome. These alternative hypotheses can be distinguished by evaluating the effect of blocking

exocytosis on phagosomal formation. To selectively inhibit secretion, we microinjected cells with either TeTx-LC or botulinum B toxin. In a variety of systems, these metalloproteases have been shown to specifically degrade v-SNARE molecules, typified by VAMP-2 (12, 14).

As shown in Fig. 2C, VAMP-2 is present in J774 cells, where it distributes in a punctate, apparently vesicular pattern. To test whether vesicular VAMP-2 is required for phagocytosis, we introduced the light chains of either tetanus or botulinum B toxin into macrophages. Because J774 cells lack receptors for these toxins, they were introduced by microinjection. Microinjection of TeTx-LC (Fig. 2A–C) or botulinum B toxin (data not shown) resulted in a marked diminution of VAMP-2 immunostaining in J774 cells, consistent with degradation of the v-SNARE. Importantly, proteolysis of VAMP-2 was associated with a significant reduction in the ability of J774 cells to undertake phagocytosis of IgG-opsonized SRBCs (Fig. 2D–F). In the small fraction of TeTx-LC-injected cells that did perform phagocytosis ( $\approx 20\%$ ; Fig. 2F), the number of SRBCs internalized per J774 cell was significantly lower than in control cells (TeTx-LC injected,  $1 \pm 0.5$  particle/cell; mock injected,  $5 \pm 1.2$  particles/cell; control (noninjected),  $5 \pm 2$  particles/cell,  $P < 0.05$  by ANOVA). By contrast, microinjection with buffer alone had no effect on either VAMP-2 immunostaining (data not shown) or phagocytosis (*insets*, Fig. 2D–F). Importantly, the inhibition of phagocytosis by TeTx-LC was not dependent on particle size, as phagocytosis

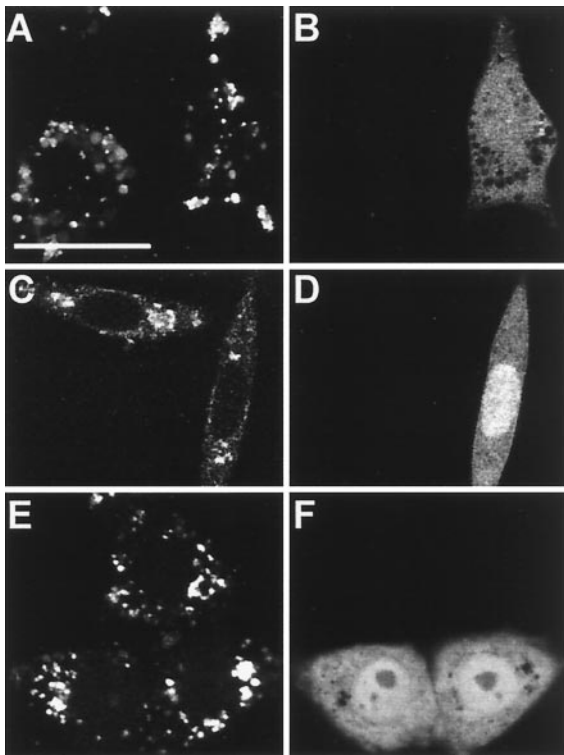


FIG. 4. Effect of tetanus toxin on endocytosis. (A and B) J774 cells were injected with TeTx-LC and fluorescein-dextran as an injection marker, incubated for 5 h at 37°C, and then allowed to internalize Texas red-dextran for 2 h at 37°C. (A) Typical confocal micrograph demonstrating Texas red fluorescence. (B) Fluorescein-dextran emission identifying injected cell. (C–F) Fc $\gamma$ RIIA-expressing CHO cells were transiently transfected with cDNA for TeTx-LC and GFP and allowed to internalize either rhodamine-labeled transferrin (C and D) or tetramethylrhodamine B isothiocyanate-labeled aggregated human IgG (E and F) for 1 h at 37°C. (C and E) Confocal fluorescence micrograph illustrating the distribution of transferrin (C) or aggregated IgG (E). (D and F) GFP emission identifying transfected cells. Representative of three experiments, with at least 50 injected or transfected cells per experiment. Bar, 10  $\mu$ m.

of very small particles, namely, *Micrococcus lysodeikticus*, was also significantly reduced after TeTx-LC injection ( $28 \pm 7\%$  of untreated cells internalized particles, compared with  $24 \pm 6\%$  in buffer-injected and only  $10 \pm 6\%$  in TeTx-LC-injected cells;  $P < 0.05$  by ANOVA).

The effects of TeTx-LC were not limited to Fc $\gamma$  receptor-mediated phagocytosis. This was concluded from studies of phagocytosis of either unopsonized zymosan or zymosan particles opsonized with serum obtained from an agammaglobulinemic patient. Internalization of unopsonized zymosan, which is thought to be mediated by receptors for mannose and other carbohydrate moieties (21), was significantly reduced after treatment with TeTx-LC ( $50 \pm 5\%$  of untreated cells internalized particles, compared with  $58 \pm 4\%$  in buffer-injected and only  $15 \pm 3\%$  in TeTx-LC-injected cells;  $P < 0.05$  by ANOVA). Similar results were obtained using particles exposed to agammaglobulinemic serum, which were opsonized by complement (control,  $57 \pm 5\%$ ; buffer injected,  $50 \pm 4\%$ ; TeTx-LC injected,  $18 \pm 5\%$ ;  $P < 0.05$ ).

Treatment with the toxins inhibited the internalization of SRBCs, but not their interaction with receptors on the surface of macrophages. This was indicated by measurements of IgG-coated SRBC adherence to J774 cells performed at 4°C to prevent phagocytosis. Under these conditions, adherence of IgG-opsonized SRBCs was indistinguishable in control and toxin-injected cells (Fig. 2, G–I). Such adherence is absent in unopsonized SRBCs (not shown), indicating that the binding

of IgG-opsonized SRBCs is mediated by Fc $\gamma$  receptors. These findings argue that VAMP-2 is required for phagocytosis at a step downstream of receptor ligation, most likely by modulating the delivery of endomembranes to the forming phagosome.

**Exocytosis Is Also Required for Phagocytosis in CHO-Fc $\gamma$ RIIA Cells.** Transfection of toxins was used to rule out possible alternate effects of the microinjection procedure. Because myeloid cells are refractory to transfection, we utilized CHO cells which had been stably transfected with the Fc $\gamma$  receptor Fc $\gamma$ RIIA (CHO-Fc $\gamma$ RIIA cells). Transfection of Fc $\gamma$ RIIA confers phagocytic properties to these cells, which are otherwise unable to perform phagocytosis (17). CHO cells that stably expressed Fc $\gamma$ RIIA receptors were transiently cotransfected with plasmids encoding TeTx-LC to degrade VAMP-2 and GFP to serve as a marker for transfection. As shown in Fig. 3, CHO-Fc $\gamma$ RIIA cells express VAMP-2, which is visible by immunofluorescence, accompanied by the presence of a cross-reacting nuclear epitope (Fig. 3 A and B). Transfection of TeTx-LC markedly diminished the punctate, cytoplasmic fluorescence associated with VAMP-2 (Fig. 3 C and D). Interestingly, while more than 30% of the control cells were able to perform phagocytosis of opsonized SRBCs, only  $15 \pm 4\%$  of TeTx-LC-transfected cells internalized IgG-coated SRBCs (Fig. 3 E–G), representing a 50% inhibition of phagocytosis. Transfection with GFP cDNA alone did not impair phagocytosis (Fig. 3 E and F insets and G). In agreement with the results obtained with macrophages, adherence of IgG-opsonized SRBCs was similar in control and TeTx-LC-transfected cells (Fig. 3G). These observations confirm that a tetanus toxin-sensitive protein, likely VAMP-2, is required for Fc $\gamma$  receptor-mediated phagocytosis in several cell types.

**Effects of Tetanus and Botulinum Toxins on Endocytosis.** It could be argued that tetanus and botulinum toxins exert nonspecific effects on membrane traffic. To assess this possibility, we examined the effect of TeTx-LC injection or transfection on endocytosis. Fig. 4 A and B shows that fluid-phase uptake by J774 cells, monitored using Texas red-dextran, was unaffected by microinjection of TeTx-LC under conditions which inhibited phagocytosis. This was confirmed by quantifying the digitized fluorescence of injected and noninjected cells using Metamorph software (noninjected,  $86 \pm 15$  fluorescence units/cell vs. injected  $80 \pm 24$  units/cell, not significant). Similarly, transfection of TeTx-LC cDNA did not alter the endocytosis of transferrin by Fc $\gamma$ RIIA-expressing CHO cells (Fig. 4 C and D). Moreover, although Fc $\gamma$  receptor mediated-phagocytosis was inhibited by TeTx-LC, internalization of aggregated IgG was unaffected (Fig. 4 E and F). This confirms that the Fc $\gamma$  receptors are available at the surface and also indicates that endocytosis, a process requiring only invagination of small domains of the plasma membrane, is unaffected by degradation of VAMP-2. Moreover, these findings imply that the effects of the toxins on phagocytosis are specific.

## DISCUSSION

Our studies provide evidence that exocytosis is required for optimal phagocytosis, and that this effect is relevant to both IgG- and non-IgG-opsonized particles. Moreover, the exocytic process is mediated by proteins like VAMP-2, which have established roles in regulated secretion in other tissues. In this regard, an effect of tetanus or botulinum toxins on VAMP homologues, including cellubrevin, cannot be excluded, although our attempts to detect VAMP-1 and cellubrevin in leukocytes using the available antibodies have thus far been unsuccessful.

It is possible that insertion of endomembranes at or near the site of phagocytosis is required for particle internalization to be successfully completed. Recent morphologic studies demonstrated the presence of lucent vesicles in the region of the phagocytic cups, which accumulate when phagocytosis is in-

hibited (22). These were formed partly by invagination of the plasmalemma, as they contained extracellular space markers. Because simply recycling plasmalemma to the site of phagocytosis could not account for the insertion of additional membrane required for surface homeostasis (see above), one could speculate that the internalized plasmalemma may fuse with endomembranes before reinsertion into the phagocytic cup. Further evidence that exocytosis of endovesicles provides the source of membrane to the nascent phagosome is derived from earlier studies in both neutrophils, which degranulate before and during phagocytosis (23), and in macrophages, where the area of membrane internalized was found by Petty *et al.* (24) to be greater than the net change in surface area. Importantly, secretory vesicles and tertiary granules of neutrophils have been demonstrated to express VAMP-2 (25). Clearly, to maintain or increase the cell area during phagocytosis, the insertion of endomembranes may occur either at the site of particle engulfment or at an alternate, remote site. Definition of the precise site of exocytosis will have to await identification of the vesicular pool of membranes secreted and of unique epitopes therein.

In conclusion, we have demonstrated that additional membrane is inserted onto the plasmalemma during the course of phagocytosis, not only compensating for the predicted loss in cell surface, but in fact resulting in a net gain in area. Moreover, such insertion of endomembranes appears to be essential for the optimal completion of phagocytosis and appears to require VAMP-2 or a related v-SNARE. These findings complement the current zipper hypothesis, which stipulates that phagosome formation results primarily from the receptor-mediated apposition of the plasma membrane to the surface of the engulfed particle. Our alternative model involving endomembrane secretion more readily accounts for the reported internalization of large or multiple particles whose net surface area approaches and sometimes exceeds that of the phagocyte plasmalemma. Moreover, a requirement for membrane fusion in phagocytosis may explain the known sensitivity of phagocytosis to wortmannin (26). This inhibitor of phosphatidylinositol 3'-kinase is known to disrupt membrane traffic in a variety of systems (27–29) and thus may interfere with phagocytosis by impairing the delivery of new membrane to the cell surface.

We thank Dr. Chaim Roifman for the generous gift of agammaglobulinemic sera. This work was supported by the Medical Research Council of Canada and the National Sanatorium Association. D.J.H. is a recipient of a postdoctoral fellowship from the Medical Research Council and an Ethicon-Society of University Surgeons Award. S.G. is an International Scholar of the Howard Hughes Medical Institute and is the current holder of the Pitblado chair in Cell Biology, the Hospital for Sick Children.

- Greenberg, S. & Silverstein, S. C. (1993) in *Phagocytosis*, ed. Paul, W. E. (Raven, New York), pp. 941–964.

- Desjardins, M., Huber, L. A., Parton, R. G. & Griffiths, G. (1994) *J. Cell Biol.* **124**, 677–688.
- Hackam, D. J., Rotstein, O. D., Zhang, W. J., Demaurex, N., Woodside, M., Tsai, O. & Grinstein, S. (1997) *J. Biol. Chem.* **272**, 29810–29820.
- Griffin, F. M., Jr., Griffin, J. A., Leider, J. E. & Silverstein, S. C. (1975) *J. Exp. Med.* **142**, 1263–1282.
- Griffin, F. M., Jr., Griffin, J. A. & Silverstein, S. C. (1976) *J. Exp. Med.* **144**, 788–809.
- Buys, S. S., Keogh, E. A. & Kaplan, J. (1984) *Cell* **38**, 569–576.
- Sollner, T., Whiteheart, S. W., Brunner, M., Erdjument-Bromage, H., Geromanos, S., Tempst, P. & Rothman, J. E. (1993) *Nature (London)* **362**, 318–324.
- Trimble, W. S., Cowan, D. M. & Scheller, R. H. (1988) *Proc. Natl. Acad. Sci. USA* **85**, 4538–4542.
- Wilson, D. W., Whiteheart, S. W., Wiedmann, M., Brunner, M. & Rothman, J. E. (1992) *J. Cell Biol.* **117**, 531–538.
- Bennett, M. K., Garcia-Ararras, J. E., Elferink, L. A., Peterson, K., Fleming, A. M., Hazuka, C. D. & Scheller, R. H. (1993) *Cell* **74**, 864–873.
- Sollner, T., Bennett, M. K., Whiteheart, S. W., Scheller, R. H. & Rothman, J. E. (1993) *Cell* **75**, 409–418.
- Schiavo, G., Benfenati, F., Poulain, B., Rossetto, O., Polverino de Lauro, P., DasGupta, B. R. & Montecucco, C. (1992) *Nature (London)* **359**, 832–835.
- Jahn, R. & Niemann, H. (1994) *Ann. N. Y. Acad. Sci.* **733**, 245–255.
- Yamasaki, S., Baumeister, A., Binz, T., Link, E., Cornille, F., Roques, B., Fykse, E. M., Sudhof, T. C., Jahn, R. & Niemann, H. (1994) *J. Biol. Chem.* **269**, 12764–12772.
- Gaisano, H. Y., Sheu, L., Foskett, J. K. & Trimble, W. S. (1994) *J. Biol. Chem.* **269**, 17062–17066.
- Richard, S., Shaw, A. S., Showell, H. J. & Connelly, P. A. (1994) *Biochem. Biophys. Res. Commun.* **199**, 653–661.
- Indik, Z. K., Kelly, C., Chien, P., Levinson, A. I. & Schreiber, A. D. (1991) *J. Clin. Invest.* **88**, 1766–1771.
- Wilson, S. P. & Smith, L. A. (1997) *Anal. Biochem.* **246**, 148–150.
- Hackam, D. J., Rotstein, O. D., Schreiber, A. D., Zhang, W. J. & Grinstein, S. (1997) *J. Exp. Med.* **186**, 955–966.
- Betz, W. J. & Bewick, G. S. (1992) *Science* **255**, 200–203.
- Shepherd, V. L., Campbell, E. J., Senior, R. M. & Stahl, P. D. (1982) *J. Reticuloendothel. Soc.* **32**, 423–431.
- Lennartz, M. R., Yuen, A. F. C., McKenzie Masi, S., Russell, D. G., Buttle, K. F. & Smith, J. J. (1997) *J. Cell Sci.* **110**, 2041–1052.
- Tapper, H. & Grinstein, S. (1997) *J. Immunol.* **159**, 409–418.
- Petty, H. R., Hafeman, D. G. & McConnell, H. M. (1981) *J. Cell Biol.* **89**, 223–229.
- Brumell, J. H., Volchuk, A., Sengelov, H., Borregaard, N., Cieutat, A. M., Bainton, D. F., Grinstein, S. & Klip, A. (1995) *J. Immunol.* **155**, 5750–5759.
- Araki, N., Johnson, M. T. & Swanson, J. A. (1996) *J. Cell Biol.* **135**, 1249–1260.
- Davidson, H. W. (1995) *J. Cell Biol.* **130**, 797–805.
- Brown, W. J., DeWald, D. B., Emr, S. D., Plutner, H. & Balch, W. E. (1995) *J. Cell Biol.* **130**, 781–796.
- Spiro, D. J., Boll, W., Kirchhausen, T. & Wessling-Resnick, M. (1996) *Mol. Biol. Cell* **7**, 355–367.